Inorg. Chem. **2008**, *47*, 2811−2819

Preparation, Characterization, and Photophysical Properties of Pt−M (M = Ru, Re) Heteronuclear Complexes with 1,10-Phenanthrolineethynyl Ligands

Yang Fan,[†] Li-Yi Zhang,[†] Feng-Rong Dai,[†] Lin-Xi Shi,[†] and Zhong-Ning Chen*[,†,‡]

State Key Laboratory of Structural Chemistry, Fujian Institute of Research on the Structure of Matter and Graduate School, Chinese Academy of Sciences, Fuzhou, Fujian 350002, China, and State Key Laboratory of Coordination Chemistry, Nanjing University, Nanjing, Jiangsu 210093, China

Received October 17, 2007

When 3-ethynyl-1,10-phenanthroline (HC≡Cphen) or 3,8-diethynyl-1,10-phenanthroline (HC≡CphenC≡CH) is utilized as a bifunctional bridging ligand via stepwise molecular fabrication, a series of Pt−Ru and Pt−Re heteronuclear complexes composed of both platinum(II) terpyridyl acetylide chromophores and a $Ru(phen)(bpy)_2$/$Re(phen)(CO)_3Cl$ subunit were prepared by complexation of one or two $Pt(^tBu_3tpy)^{2+}$ units to the mononuclear Ru^{II} or Re^{I} precursor through platinum acetylide σ coordination. These Pt−Ru and Pt−Re complexes exhibit intense low-energy absorptions originating from both Pt- and Ru (Re)-based metal-to-ligand charge-transfer (MLCT) states in the near-visible region. They are strongly luminescent in both solid states and fluid solutions with a submicrosecond range of lifetimes and 0.27–6.58% of quantum yields in degassed acetonitrile. For the Pt−Ru heteronuclear complexes, effective intercomponent Pt → Ru energy transfer takes place from the platinum(II) terpyridyl acetylide chromophores to the ruthenium(II) tris(diimine)-based emitters. In contrast, dual emission from both Pt- and Re-based ^{3}MLCT excited states occurs because of less efficient intercomponent Pt → Re energy transfer in the Pt−Re heteronuclear complexes.

Introduction

The syntheses and characterization of multicomponent systems comprising electroactive and/or photoactive transition-metal subunits have attracted great attention because photoinduced intercomponent electron/energy-transfer processes play a significant role in the process of solar energy conversion.[1,7] Taking advantage of the tunable photophysical and photochemical properties, a series of transition-metal-based multicomponent complexes performing useful functions have been developed that have potential applications as optoelectronic materials at the molecular level.[2] In these heteronuclear or multicomponent species, the ruthenium(II), osmium(II), and rhenium(I) polypyridine subunits and lanthanide(III) 1,3-diketonate chromophores are frequently employed as emitters or photosensitizers, in which intercomponent electron/energy-transfer processes usually occur from the metal-to-ligand charge transfer triplet (^{3}MLCT) excited states.[3]

* To whom correspondence should be addressed. E-mail: czn@fjirsm.ac.cn.
† Chinese Academy of Sciences.
‡ Nanjing University.

(1) (a) Eisenberg, R.; Nocera, D. G. *Inorg. Chem.* **2005**, *44*, 6799. (b) Gust, D.; Moore, T. A.; Moore, A. L. *Acc. Chem. Res.* **2001**, *34*, 40. (c) Alstrum-Acevedo, J. H.; Brennaman, M. K.; Meyer, T. J. *Inorg. Chem.* **2005**, *44*, 6802. (d) Meyer, G. J. *Inorg. Chem.* **2005**, *44*, 6852. (e) Dempsey, J. L.; Esswein, A. J.; Manke, D. R.; Rosenthal, J.; Soper, J. D.; Nocera, D. G. *Inorg. Chem.* **2005**, *44*, 6879. (f) Odobel, F.; Zabri, H. *Inorg. Chem.* **2005**, *44*, 5600.

(2) (a) Hissler, M.; McGarrah, J. E.; Connick, W. B.; Geiger, D. K.; Cummings, S. D.; Eisenberg, R. *Coord. Chem. Rev.* **2000**, *208*, 115. (b) Nishihara, H.; Kanaizuka, K.; Nishimori, Y.; Yamanoi, Y. *Coord. Chem. Rev.* **2007**, *251*, 2674. (c) Balzani, V. *Photochem. Photobiol. Sci.* **2003**, *2*, 459. (d) Imahori, H.; Fukuzumi, S. *Adv. Funct. Mater.* **2004**, *14*, 525. (e) Ziessel, R.; Hissler, M.; El-ghayoury, A.; Harriman, A. *Coord. Chem. Rev.* **1998**, *1251*, 178–180. (f) Ward, M. D. *Coord. Chem. Rev.* **2007**, *251*, 1663. (g) Montes, V. A.; Perez-Bolivar, C.; Agarwal, N.; Shinar, J.; Anzenbacher, P., Jr. *J. Am. Chem. Soc.* **2006**, *128*, 12436. (h) Klink, S. I.; Keizer, H.; van Veggel, F. C. J. M. *Angew. Chem., Int. Ed.* **2000**, *39*, 4319. (i) Harriman, A. *Angew. Chem., Int. Ed.* **2004**, *43*, 4985. (j) Winters, M. U.; Dahlstedt, E.; Blades, H. E.; Wilson, C. J.; Frampton, M. J.; Anderson, H. L.; Albinsson, B. *J. Am. Chem. Soc.* **2007**, *129*, 4291. (k) Nastasi, F.; Puntoriero, F.; Campagna, S.; Schergna, S.; Maggini, M.; Cardinali, F.; Delavaux-Nicot, B.; Nierengarten, J.-F. *Chem. Commun.* **2007**, 3556.

10.1021/ic702055n CCC: $40.75
Published on Web 03/01/2008

Platinum(II) terpyridyl alkynyl complexes have been extensively investigated because of their tunable spectroscopic and luminescent properties by modifying the electronic nature in both terpyridyl and alkynyl ligands.[4] Most remarkably, these species usually exhibit intense low-energy absorption in the near-visible region and long-lived room-temperature photoluminescence from ^{3}MLCT states with high quantum yields. Furthermore, the remarkable emissive features from Pt(terpyridyl)(acetylide)-based chromophores have found extensive applications in the photocatalytic generation of hydrogen,[5] chemical sensing,[6] photoinduced charge separation, [7] and singlet oxygen photosensitization.[8] Compared with numerous studies on homonuclear platinum(II) terpyridyl alkynyl complexes,[4–8] the construction of heteronuclear and multicomponent arrays based on Pt(terpyridyl)(acetylide) chromophores for the study of intercomponent energy-transfer processes, however, is much neglected because of the difficulty in controlling the arrays with two or more types of metal subunits.[9] Yam et al. described a series of rodlike heterobimetallic rhenium(I)−platinum(II) alkynyl complexes linked by 1,4-diethynylphenylene, in which the luminescence arises from Pt^{II}-based ^{3}MLCT excited states.[9a] Odobel et al. synthesized a series of diads composed of zinc or magnesium porphyrin and platinum(II) terpyridyl subunits bridged by a *p*-phenylenebis(acetylene) spacer, in which a long-range electron transfer occurs from the porphyrin chromophore to the Pt^{II} center.[9b] Recently, Ziessel et al. reported a bimetallic Pt−Eu complex (^{t}Bu$_3$tpy)Pt(C≡Ctpy)Eu(hfac)$_3$ (HC≡Ctpy = 4′-ethynyl-2,2′:6′,2″-terpyridine), in which a highly efficient d → f energy transfer is operating from the Pt(^{t}Bu$_3$tpy)(acetylide) chromophore to the Eu^{III} center so that the Pt^{II}-based subunit serves as an effective sensitizer for Eu^{III} luminescence.[9c]

We have been interested in the design of heterometallic and/or multicomponent complexes composed of two or more redox-active and/or photoactive metal subunits using polypyridyl-functionalized alkynyl ligands for the purpose of developing optoelectronic materials at the molecular level.[10] A series of heterometallic arrays with bipyridyl- or tripyridyl-functionalized alkynyl ligands have been prepared by complexation of transition-metal sensitizers and lanthanide emitters through both metal-acetylide σ coordination and bipyridy/tripyridyl chelation, respectively, where sensitized near-infrared (NIR) lanthanide luminescence is usually achieved through efficient energy transfers from transition-metal alkynyl subunits to lanthanide centers.[10b–e] In contrast, utilization of polypyridyl-functionalized alkynyl ligands for the construction of Pt−Ru and Pt−Re heterometallic arrays based on platinum(II) terpyridyl acetylide chromophores has not been investigated yet. In this paper, we describe the preparation, characterization, and photophysical properties of a series of Pt−Ru and Pt−Re heteronuclear alkynyl complexes linked by bridging 3-ethynyl-1,10-phenanthroline or 3,8-diethynyl-1,10-phenanthroline through both ruthenium/rhenium phenanthroline chelation and platinum acetylide σ coordination, in which intercomponent triplet energy transfer is operating from the platinum(II) terpyridylalkynyl chromophore to the Ru- or Re-based subunits.

Experimental Section

Materials and Reagents. All manipulations were performed under an argon atmosphere using standard Schlenk techniques and vacuum-line systems. The solvents were dried and distilled by standard procedures prior to use, except spectroscopic-grade acetonitrile from Merck was used as received for the photophysical measurements. (Trimethylsilyl)acetylene (Me_3SiC≡CH), rhenium(I) pentacarbonyl chloride [$Re(CO)_5Cl$], and copper(I) iodide (CuI) were commercially available and used as received. *cis*-Ru(bpy)$_2$Cl$_2$·2H$_2$O[11a] and 4,4′,4″-tri-*tert*-butyl-2,2′:6′,2″-terpyridine (^{t}Bu$_3$tpy)[11b] were synthesized according to the literature methods.

(3) (a) Sauvage, J. P.; Collin, J. P.; Chambron, J. C.; Guillerez, S.; Coudret, C.; Balzani, V.; Barigelletti, F.; Cola, L. D.; Flamigni, L. *Chem. Rev.* **1994**, *94*, 993. (b) Balzani, V.; Juris, A.; Venturi, M.; Campagna, S.; Serroni, S. *Chem. Rev.* **1996**, *96*, 759. (c) Hissler, M.; Harriman, A.; Khatyr, A.; Ziessel, R. *Chem.—Eur. J.* **1999**, *5*, 3366. (d) Harriman, A.; Hissler, M.; Trompette, O.; Ziessel, R. *J. Am. Chem. Soc.* **1999**, *121*, 2516. (e) Pomestchenko, I. E.; Polyansky, D. E.; Castellano, F. N. *Inorg. Chem.* **2005**, *44*, 3412. (f) Shiotsuka, M.; Yamamoto, Y.; Okuno, S.; Kitou, M.; Nozaki, K.; Onaka, S. *Chem. Commun.* **2002**, 590. (g) Harriman, A.; Hissler, M.; Ziessel, R.; Cian, A. D.; Fisher, J. *J. Chem. Soc., Dalton Trans.* **1995**, 4067. (h) Yamamoto, Y.; Shiotsuka, M.; Onaka, S. *J. Organomet. Chem.* **2004**, *689*, 2905. (i) Barigelletti, F.; Flamigni, L.; Balzani, V.; Collin, J.-P.; Sauvage, J.-P.; Sour, A.; Constable, E. C.; Cargill Thompson, A. M. W. *J. Am. Chem. Soc.* **1994**, *116*, 7692. (j) Bardwell, D. A.; Barigelletti, F.; Cleary, R. L.; Flamigni, L.; Guardigli, M.; Jeffery, J. C.; Ward, M. D. *Inorg. Chem.* **1995**, *34*, 2438. (k) Argazzi, R.; Bertolasi, E.; Chiorboli, C.; Bignozzi, C. A.; Itokazu, M. K.; Murakami Iha, N. Y. *Inorg. Chem.* **2001**, *40*, 6885. (l) Cleary, R. L.; Byrom, K. J.; Bardwell, D. A.; Jeffery, J. C.; Ward, M. D.; Calogero, G.; Armaroli, N.; Flamigni, L.; Barigelletti, F. *Inorg. Chem.* **1997**, *36*, 2601. (m) Ott, S.; Borgström, M.; Hammarström, L.; Johansson, O. *Dalton Trans.* **2006**, 1434.

(4) (a) Yam, V. W.-W.; Wong, K. M.-C.; Zhu, N. *Angew. Chem., Int. Ed.* **2003**, *42*, 1400. (b) Castellano, F. N.; Pomestchenko, I. E.; Shikhova, E.; Hua, F.; Muro, M. L.; Rajapakse, N. *Coord. Chem. Rev.* **2006**, *250*, 1819. (c) Shikhova, E.; Danilov, E. O.; Kinayyigit, S.; Pomestchenko, I. E.; Tregubov, A. D.; Camerel, F.; Retailleau, P.; Ziessel, R.; Castellano, F. N. *Inorg. Chem.* **2007**, *46*, 3038. (d) Guo, F.; Sun, W.; Liu, W.; Schanze, K. *Inorg. Chem.* **2005**, *44*, 4055.

(5) (a) Du, P.; Schneider, J.; Jarosz, P.; Eisenberg, R. *J. Am. Chem. Soc.* **2006**, *128*, 7726. (b) Zhang, D.; Wu, L.-Z.; Zhou, L.; Han, X.; Yang, Q.-Z.; Zhang, L.-P.; Tung, C.-H. *J. Am. Chem. Soc.* **2004**, *126*, 3440. (c) Du, P.; Schneider, J.; Jarosz, P.; Zhang, J.; Brennessel, W. W.; Eisenberg, R. *J. Phys. Chem. B.* **2007**, *111*, 6887.

(6) (a) Wong, K. M.-C.; Yam, V. W.-W. *Coord. Chem. Rev.* **2007**, *251*, 2477. (b) Lo, H.-S.; Yip, S.-K.; Wong, K. M.-C.; Zhu, N.; Yam, V. W.-W. *Organometallics.* **2006**, *25*, 3537. (c) Han, X.; Wu, L.-Z.; Si, G.; Pan, J.; Yang, Q.-Z.; Zhang, L.-P.; Tung, C.-H. *Chem.—Eur. J.* **2007**, *13*, 1231. (d) Fan, Y.; Zhu, Y.-M.; Dai, F.-R.; Zhang, L.-Y.; Chen, Z.-N. *Dalton Trans.* **2007**, 3885.

(7) (a) Chakraborty, S.; Wadas, T. J.; Hester, H.; Schmehl, R.; Eisenberg, R. *Inorg. Chem.* **2005**, *44*, 6865. (b) Chakraborty, S.; Wadas, T. J.; Hester, H.; Flaschenreim, C.; Schmehl, R.; Eisenberg, R. *Inorg. Chem.* **2005**, *44*, 6284.

(8) Zhang, D.; Wu, L.-Z.; Yang, Q.-Z.; Li, X.-H.; Zhang, L.-P.; Tung, C.-H. *Org. Lett.* **2003**, *5*, 3221.

(9) (a) Lam, S. C.-F.; Yam, V. W.-W.; Wong, K. M.-C.; Cheng, E. C.-C.; Zhu, N. *Organometallics* **2005**, *24*, 4298. (b) Monnereau, C.; Gomez, J.; Blart, E.; Odobel, F.; Wallin, S.; Fallberg, A.; Hammarstrom, L. *Inorg. Chem.* **2005**, *44*, 4806. (c) Ziessel, R.; Diring, S.; Kadjane, P.; Charbonnière, L.; Retailleau, P.; Philouze, C. *Chem. Asian J.* **2007**, *2*, 975. (d) Ziessel, R.; Diring, S.; Retailleau, P. *Dalton Trans.* **2006**, 3285.

(10) (a) Wei, Q.-H.; Yin, G.-Q.; Zhang, L.-Y.; Chen, Z.-N. *Inorg. Chem.* **2006**, *45*, 10371. (b) Xu, H.-B.; Shi, L.-X.; Ma, E.; Zhang, L.-Y.; Wei, Q.-H.; Chen, Z.-N. *Chem. Commun.* **2006**, 1601. (c) Xu, H.-B.; Zhang, L.-Y.; Xie, Z.-L.; Ma, E.; Chen, Z.-N. *Chem. Commun.* **2007**, 2744. (d) Li, X.-L.; Dai, F.-R.; Zhang, L.-Y.; Zhu, Y.-M.; Peng, Q.; Chen, Z.-N. *Organometallics* **2007**, *26*, 4483. (e) Li, X.-L.; Shi, L.-X.; Zhang, L.-Y.; Wen, H.-M.; Chen, Z.-N. *Inorg. Chem.* **2007**, *48*, 10892. (f) Xu, H.-B.; Zhang, L.-Y.; Chen, Z.-N. *Inorg. Chim. Acta* **2007**, *360*, 163.

[Pt(ᵗBu₃tpy)Cl](PF₆),[11c] 3-bromo-1,10-phenanthroline, 3,8-dibromo-1,10-phenanthroline,[11d] 3-(trimethylsilyl)ethynyl-1,10-phenanthroline,[14a] and 3,8-di[(trimethylsilyl)ethynyl]-1,10-phenanthroline[14b] were synthesized by modification of the procedures described in the literature. The analogous of the mononuclear Ru^{II} and Re^{I} complexes **1**−**4** containing −C≡CH instead of −C≡CSiMe₃ groups have already been described in the literature.[3h,11d,e]

3-(Trimethylsilyl)ethynyl-1,10-phenanthroline (phenC≡CSiMe₃). A mixture of 3-bromo-1,10-phenanthroline (1.0 g, 3.86 mmol), (trimethylsilyl)acetylene (0.67 mL, 4.63 mmol), $Pd(PPh_3)_2Cl_2$ (135 mg, 0.19 mmol), and CuI (36 mg, 0.19 mmol) in a tetrahydrofuran−diisopropylamine [60 mL, 2:1 (v/v)] solution was refluxed for 12 h. After cooling to room temperature, the reaction mixture was filtered, and the filtrate was evaporated to dryness under reduced pressure to give a solid residue. The crude product was purified by column chromatography on silica gel using dichloromethane−methanol [100:1 (v/v)] as the eluent. Yield: 76%. Anal. Calcd for $C_{17}H_{16}N_2Si$: C, 73.87; H, 5.83; N, 10.13. Found: C, 73.82; H, 5.85; N, 10.11. ESI-MS (*m*/*z*): 277.2 $[M + H]^+$. ^1H NMR ($CHCl_3$-*d*): 9.21 (d, J = 5.2 Hz, 1H, phen), 9.20 (s, 1H, phen), 8.34 (d, J = 2.0 Hz, 1H, phen), 8.26 (dd, J_1 = 1.2 Hz, J_2 = 1.2 Hz, 1H, phen), 7.81 (d, J = 8.8 Hz, 1H, phen), 7.74 (d, J = 9.2 Hz, 1H, phen), 7.66 (dd, J_1 = 4.4 Hz, J_2 = 4.4 Hz, 1H, phen), 0.32 (s, 9H, CH_3). IR (KBr disk, ν/cm^{-1}): 2153s (C≡C).

3,8-Di[(trimethylsilyl)ethynyl]-1,10-phenanthroline (Me₃SiC≡CphenC≡CSiMe₃). This compound was prepared by the same synthetic procedure as that of 3-(trimethylsilyl)ethynyl-1,10-phenanthroline except that 3,8-dibromo-1,10-phenanthroline (0.5 g, 1.48 mmol) was used in place of 3-bromo-1,10-phenanthroline. The crude product was purified by column chromatography on silica gel using dichloromethane as the eluent. Yield: 83%. Anal. Calcd for $C_{22}H_{24}N_2Si_2$: C, 70.92; H, 6.49; N, 7.52. Found: C, 70.96; H, 6.46; N, 7.53. ESI-MS (*m*/*z*): 373.4 $[M + H]^+$. ^1H NMR ($CHCl_3$-*d*): 9.19 (s, 2H, phen), 8.32 (d, J = 1.6 Hz, 2H, phen), 7.74 (s, 2H, phen), 0.32 (s, 18H, CH_3). IR (KBr disk, ν/cm^{-1}): 2150s (C≡C).

[Ru(bpy)₂(phenC≡CSiMe₃)](PF₆)₂ (1). A mixture of *cis*-$Ru(bpy)_2Cl_2 \cdot 2H_2O$ (500 mg, 0.96 mmol) and phenC≡CSiMe₃ (358 mg, 0.96 mmol) in absolute ethanol (50 mL) was refluxed for 12 h. After cooling to room temperature, a methanol (10 mL) solution of NH_4PF_6 (500 mg) was added to the above solution with stirring for 30 min. The solution was then evaporated to dryness under reduced pressure, giving a solid residue that was extracted with dichloromethane. The crude product was purified by chromatography on an alumina column using dichloromethane−methanol (100:0.5) as the eluent. Yield: 70%. Anal. Calcd for $C_{37}H_{32}F_{12}N_6P_2SiRu$: C, 45.36; H, 3.29; N, 8.58. Found: C, 45.31; H, 3.27; N, 8.56. ESI-MS (*m*/*z*): 345.1 $[M - 2PF_6]^{2+}$, 835.1 $[M - PF_6]^+$. ^1H NMR (CH_3CN-d_3): 8.66 (s, 1H), 8.62 (d, J = 8.0 Hz, 2H), 8.52 (d, J = 5.0 Hz, 2H), 8.49 (d, J = 8.5 Hz, 2H), 8.26 (d, J = 9.0 Hz, 1H), 8.21 (d, J = 7.5 Hz, 1H), 8.10 (d, J = 9.0 Hz, 2H), 8.02 (d, J = 7.0 Hz, 2H), 7.85 (d, J = 5.0 Hz, 1H), 7.79 (d, J = 5.0 Hz, 1H), 7.74 (d, J = 2.0 Hz, 1H), 7.61 (d, J = 2.0 Hz, 2H), 7.49 (d, J = 2.0 Hz, 1H), 7.46 (d, J = 5.5 Hz, 2H), 7.24 (s, 2H), 0.24 (s, 9H, CH_3). IR (KBr disk, ν/cm^{-1}): 2159w (C≡C).

Re(phenC≡CSiMe₃)(CO)₃Cl (2). A mixture of $Re(CO)_5Cl$ (180 mg, 0.50 mmol) and phenC≡CSiMe₃ (138 mg, 0.50 mmol) in toluene (30 mL) was refluxed for 8 h under an argon atmosphere. After cooling to room temperature, the resulting orange precipitate was filtered off, washed with hexane and ether, and dried in vacuum. Yield: 75%. Anal. Calcd for $C_{20}H_{16}ClN_2O_3SiRe$: C, 41.27; H, 2.77; N, 4.81. Found: C, 41.31; H, 2.79; N, 4.76. ESI-MS (*m*/*z*): 582.1 $[M]^+$. ^1H NMR (CH_3CN-d_3): 9.40 (s, 1H, phen), 9.34 (s, 1H, phen), 8.77 (s, 1H, phen), 8.76 (s, 1H, phen), 8.20 (d, J = 8.5 Hz, 1H, phen), 8.12 (d, J = 8.0 Hz, 1H, phen), 7.99 (s, 1H, phen), 0.35 (s, 9H, CH_3). IR (KBr disk, ν/cm^{-1}): 2159w (C≡C), 2022s (CO), 1927s (CO), 1888s (CO).

[Ru(bpy)₂(Me₃SiC≡CphenC≡CSiMe₃)](PF₆)₂ (3). This compound was prepared by the same synthetic procedure as that of **1** except that Me₃SiC≡CphenC≡CSiMe₃ (358 mg, 0.96 mmol) was used in place of phenC≡CSiMe₃. The crude product was purified by chromatography on an alumina column using dichloromethane−methanol (100:1) as the eluent. Yield: 70%. Anal. Calcd for $C_{42}H_{40}F_{12}N_6P_2Si_2Ru$: C, 46.88; H, 3.75; N, 7.81. Found: C, 46.82; H, 3.79; N, 7.84. ESI-MS (*m*/*z*): 393.1 $[M - 2PF_6]^{2+}$, 931.0 $[M - PF_6]^+$. ^1H NMR (CH_3CN-d_3): 8.96 (s, 2H), 8.84 (d, J = 8.0 Hz, 2H), 8.81 (d, J = 8.0 Hz, 2H), 8.33 (s, 2H), 8.20 (d, J = 4.0 Hz, 2H), 8.12 (d, J = 4.0 Hz, 2H), 7.98 (s, 2H), 7.76 (d, J = 2.0 Hz, 2H), 7.64 (d, J = 2.0 Hz, 2H), 7.58 (d, J = 4.0 Hz, 2H), 7.35 (d, J = 2.0 Hz, 2H), 0.22 (s, 18H, CH_3). IR (KBr disk, ν/cm^{-1}): 2158w (C≡C).

Re(Me₃SiC≡CphenC≡CSiMe₃)(CO)₃Cl (4). This compound was prepared by the same synthetic procedure as that of **2** except that Me₃SiC≡CphenC≡CSiMe₃ (186 mg, 0.50 mg) was used instead of phenC≡CSiMe₃. Yield: 72%. Anal. Calcd for $C_{25}H_{24}ClN_2O_3Si_2Re$: C, 44.27; H, 3.57; N, 4.13. Found: C, 44.33; H, 3.55; N, 4.16. ESI-MS (*m*/*z*): 678.9 $[M]^+$. ^1H NMR (DMSO-d_6): 9.35 (s, 2H, phen), 9.14 (s, 2H, phen), 8.28 (s, 2H, phen), 0.34 (s, 18H, CH_3). IR (KBr disk, ν/cm^{-1}): 2159w (C≡C); 2025 (CO), 1924 (CO), 1885 (CO).

[{Ru(bpy)₂}{Pt(ᵗBu₃tpy)}(phenC≡C)](PF₆)₃ (5). A mixture of **1** (489 mg, 0.5 mmol), [Pt(ᵗButpy)Cl](PF₆) (388 mg, 0.5 mmol), CuI (5 mg, 0.025 mmol), and KF (87 mg, 1.5 mmol) in a dichloromethane−methanol solution [60 mL, 2:1 (v/v)] was refluxed for 1 day. After cooling to room temperature, the solution was evaporated to dryness under reduced pressure. The solid residue was extracted with dichloromethane and the solution evaporated to dryness under reduced pressure to give a crude product that was purified by chromatography on an alumina column using dichloromethane−methanol (100:0.5) as the eluent. Yield: 65%. Anal. Calcd for $C_{61}H_{58}F_{18}N_9P_3PtRu$: C, 44.45; H, 3.55; N, 7.65. Found: C, 44.41; H, 3.58; N, 7.62. ESI-MS (*m*/*z*): 404.4 $[M - 3PF_6]^{3+}$, 679.8 $[M - 2PF_6]^{2+}$. ^1H NMR (CH_3CN-d_3): 8.95 (d, J = 6.0 Hz, 1H), 8.67 (s, 2H), 8.63 (d, J = 8.0 Hz, 2H), 8.54 (d, J = 7.5 Hz, 2H), 8.39 (s, 2H), 8.36 (s, 2H), 8.24 (d, J = 4.0 Hz, 2H), 8.20 (s, 1H), 8.12 (d, J = 4.0 Hz, 1H), 8.07 (d, J = 4.5 Hz, 2H), 8.04 (s, 1H), 7.94 (s, 1H), 7.82 (s, 1H), 7.73 (d, J = 2.0 Hz, 2H), 7.71 (d, J = 2.0 Hz, 2H), 7.65 (d, J = 2.0 Hz, 1H), 7.57 (d, J = 4.0 Hz, 2H), 7.48 (d, J = 2.0 Hz, 2H), 7.28 (d, J = 2.0 Hz, 2H), 1.57 (s, 9H, CH_3), 1.50 (s, 18H, CH_3). IR (KBr disk, ν/cm^{-1}): 2110s (C≡C).

[{Re(CO)₃Cl}{Pt(ᵗBu₃tpy)}(phenC≡C)](PF₆) (6). This compound was prepared by the same synthetic procedure as that of **5** except that **2** (291 mg, 0.50 mmol) was used in place of **1**. The crude product was purified by chromatography on an alumina column using dichloromethane−methanol (100:0.5) as the eluent. Yield: 71%. Anal. Calcd for $C_{44}H_{42}ClF_6N_5O_3PPtRe$: C, 42.26; H, 3.39; N, 5.60. Found: C, 42.31; H, 3.42; N, 5.53. ESI-MS (*m*/*z*): 1106.0 $[M - PF_6]^+$. ^1H NMR (DMSO-d_6): 9.40 (d, J = 5.2 Hz, 1H, phen), 9.35 (s, 1H, phen), 9.06 (d, J = 5.0 Hz, 2H, tpy), 8.96 (s, 1H, phen), 8.89 (d, J = 8.0 Hz, 1H, phen), 8.70 (s, 4H, tpy), 8.22 (d, J = 8.8 Hz, 1H, phen), 8.15 (d, J = 8.4 Hz, 1H, phen), 8.05 (d, J = 7.6 Hz, 1H, phen), 7.83 (d, J = 5.6 Hz, 2H, tpy), 1.54 (s, 9H, CH_3), 1.44 (s, 18H, CH_3). IR (KBr disk, ν/cm^{-1}): 2112w (C≡C), 2019 (CO), 1921 (CO), 1892 (CO).

[Pt(ᵗBu₃tpy)(phenC≡C)](PF₆) (7). A mixture of [Pt(ᵗBu₃tpy)Cl](PF₆) (388 mg, 0.5 mmol), phenC≡CSiMe₃ (138 mg, 0.5 mmol), CuI (2 mg, 0.01 mmol), and KF (87 mg, 1.5 mmol) in a

dichloromethane−methanol solution [60 mL, 2:1 (v/v)] was refluxed for 1 day. After cooling to room temperature, the solution was evaporated to dryness under reduced pressure to give a solid residue that was washed with water, ethanol, and dichloromethane. The product was purified by recrystallization from MeCN/Et_2O. Yield: 63%. Anal. Calcd for $C_{41}H_{42}N_5F_6PPt$: C, 52.12; H, 4.48; N, 7.41. Found: C, 52.09; H, 4.50; N, 7.35. ESI-MS (*m*/*z*): 799.3 [M − PF_6]$^+$. ^{1}H NMR (DMSO-d_6): 8.91 (d, J = 5.6 Hz, 1H, phen), 8.86 (d, J = 9.0 Hz, 2H, tpy), 8.78 (s, 4H, tpy), 8.30 (s, 1H, phen), 8.20 (d, J = 7.6 Hz, 1H, phen), 7.98 (s, 2H, phen), 7.91 (d, J = 4.8 Hz, 2H, tpy), 7.77 (s, 1H, phen), 7.73 (d, J = 5.6 Hz, 1H, phen), 1.54 (s, 9H, CH_3), 1.48 (s, 18H, CH_3). IR (KBr disk, ν/cm^{-1}): 2118s (C≡C).

[{(^{t}Bu$_3$tpy)Pt}$_2$(C≡CphenC≡C)](PF$_6$)$_2$ (8). This compound was prepared by the same synthetic procedure as that of **7** except that Me_3SiC≡CphenC≡$CSiMe_3$ (68 mg, 0.20 mmol) was used in place of phenC≡$CSiMe_3$. The crude product was purified by chromatography on an alumina column using dichloromethane−methanol (100:1) as the eluent. Yield: 76%. Anal. Calcd for $C_{70}H_{76}F_{12}N_8P_2Pt_2$: C, 49.18; H, 4.48, N, 6.55. Found: C, 49.22; H, 4.45, N, 6.61. ESI-MS (*m*/*z*): 709.4 [M − 2PF_6]$^{2+}$, 1563.9 [M − PF_6]$^+$. ^{1}H NMR (DMSO-d_6): 9.14 (s, 2H, phen), 9.11 (d, J = 5.6 Hz, 4H, tpy), 8.70 (s, 8H, tpy), 8.44 (s, 2H, phen), 7.92 (d, J = 5.6 Hz, 4H, tpy), 7.88 (s, 2H, phen), 1.55 (s, 18H, CH_3), 1.47 (s, 36H, CH_3). IR (KBr disk, ν/cm^{-1}): 2113s (C≡C).

[{Ru(bpy)$_2$}{(^{t}Bu$_3$tpy)Pt}$_2$(C≡CphenC≡C)](PF$_6$)$_4$ (9). This compound was prepared by the same synthetic procedure as that of **5** except that **3** (538 mg, 0.5 mmol) was used in place of **1**. The crude product was purified by chromatography on an alumina column using dichloromethane−methanol (100:1) as the eluent. Yield: 67%. Anal. Calcd for $C_{90}H_{92}F_{24}N_{12}P_4Pt_2Ru$: C, 44.80; H, 3.84, N, 6.97. Found: C, 44.83; H, 3.82, N, 6.94. ESI-MS (*m*/*z*): 458.3 [M − 4PF_6]$^{4+}$, 1061.9 [M − 2PF_6]$^{2+}$, 659.4 [M − 3PF_6]$^{3+}$. ^{1}H NMR (CH_3CN-d_3): 8.95 (d, J = 6.0 Hz, 2H), 8.66 (s, 2H), 8.57 (s, 4H), 8.56 (s, 2H), 8.39 (s, 4H), 8.36 (s, 4H), 8.19 (s, 2H), 8.09 (s, 2H), 8.08 (s, 2H), 8.06 (s, 2H), 7.90 (s, 4H), 7.73 (s, 2H), 7.66 (d, J = 2.0 Hz, 2H), 7.50 (s, 2H), 7.35 (s, 2H), 1.57 (s, 18H, CH_3), 1.50 (s, 36H, CH_3). IR (KBr disk, ν/cm^{-1}): 2113s (C≡C).

[{Re(CO)$_3$Cl}{(^{t}Bu$_3$tpy)Pt}$_2$(C≡CphenC≡C)](PF$_6$)$_2$ (10). This compound was prepared by the same synthetic procedure as that of **5** except that **4** (135 mg, 0.2 mmol) was used in place of **1**. The crude product was purified by chromatography on an alumina column using dichloromethane−methanol (100:1) as the eluent. Yield: 65%. Anal. Calcd for $C_{73}H_{76}ClF_{12}N_8O_3P_2Pt_2Re$: C, 43.51; H, 3.80; N, 5.56. Found: C, 43.52; H, 3.76; N, 5.62. ESI-MS (*m*/*z*): 862.3 [M − 2PF_6]$^{2+}$. ^{1}H NMR (DMSO-d_6): 9.26 (s, 2H, phen), 9.09 (s, 4H, tpy), 8.67 (s, 2H, phen), 8.62 (s, 4H, tpy), 8.60 (s, J = 8.8 Hz, 4H, tpy), 7.85 (s, 2H, phen), 7.78 (s, 4H, tpy), 1.52 (s, 18H, CH_3), 1.45 (s, 36H, CH_3). IR (KBr disk, ν/cm^{-1}): 2114s (C≡C), 2025 (CO), 1929 (CO), 1889 (CO).

Physical Measurements. Elemental analyses (C, H, N) were performed on a Perkin-Elmer model 240C automatic instrument. Electrospay ion mass spectra (ESI-MS) were recorded on a Finnigan LCQ mass spectrometer using dichloromethane−methanol as the mobile phase. UV–vis absorption spectra were measured on a Perkin-Elmer Lambda 25 UV–vis spectrometer. IR spectra were recorded on a Magna 750 FT-IR spectrophotometer with KBr pellets. ^{1}H NMR spectra were measured on a Varian UNITY-500 spectrometer with $SiMe_4$ as the internal reference. Emission and excitation spectra were recorded on a Perkin-Elmer LS55 luminescence spectrometer with a R928 red-sensitive photomultiplier. Emission lifetimes in solid states and degassed solutions were determined on an Edinburgh Analytical Instrument (F900 fluorescence spectrometer), and the resulting emission was detected by a thermoelectrically cooled Hamamatsu R3809 photomultiplier tube. The instrument response function at the excitation wavelength was deconvolved from the luminescence decay. Emission quantum yields were measured in degassed acetonitrile solutions at 298 K by the method of Demas and Crosby.[12] A degassed acetonitrile solution of [Ru(bpy)$_3$]Cl_2 (bpy = 2,2′-bipyridine) was used as the standard (φ_{em} = 0.062). The cyclic voltammogram (CV) and differential pulse voltammogram (DPV) were made with a potentiostat/galvanostat model 263A in acetonitrile solutions containing 0.1 M Bu_4NPF_6 as the supporting electrolyte. The CV was performed at a scan rate of 200 mV s^{-1}. The DPV was measured at a rate of 20 mV s^{-1} with a pulse height of 40 mV. Platinum and glassy graphite were used as the counter and working electrodes, respectively, and the potential was measured against a Ag/AgCl reference electrode. The potential measured was always referenced to the half-wave potentials of the ferrocenium/ferrocene couple ($E_{1/2}$ = 0).

Crystal Structure Determination. Single crystals of **9**·5½H_2O were obtained by diffusion of isopropyl ether into an acetonitrile solution. A single crystal sealed in a capillary with mother liquor was measured on a Rigaku Mercury CCD diffractometer by the ω-scan technique at room temperature using graphite-monochromated Mo Kα (λ = 0.710 73 Å) radiation. The *CrystalClear* software package was used for data reduction and empirical absorption correction. The structure was solved by direct methods, and the heavy atoms were located from an E map. The remaining non-hydrogen atoms were determined from the successive difference Fourier syntheses. All non-hydrogen atoms were refined anisotropically, and the hydrogen atoms were generated geometrically and refined with isotropic thermal parameters. The structure was refined on F^2 by full-matrix least-squares methods using the *SHELXTL-97* program package.[13] The crystallographic data of **9** are summarized in Table 1.

Table 1. Crystallographic Data for **9**·5½H_2O

	9·5½H_2O
compound	$C_{90}H_{103}F_{24}N_{12}O_{5.5}P_4Pt_2Ru$
empirical formula	2511.97
temp, K	293(2)
space group	*C*2/*c*
a, Å	26.894(12)
b, Å	31.142(12)
c, Å	26.595(11)
β, deg	96.057(1)
V, Å^3	22150(16)
Z	8
ρ_{calcd}, g/cm^{-3}	1.507
μ, mm^{-1}	2.804
radiation (λ, Å)	0.710 73
R1 (F_o)[a]	0.0647
wR2 (F_o)[b]	0.1999
GOF	1.095

[a] R1 = $\sum|F_o - F_c|/\sum F_o$ [b] wR2 = $\sum[w(F_o^2 - F_c^2)^2]/\sum[w(F_o^2)]^{1/2}$.

Results and Discussion

Syntheses and Characterization. 3-(Trimethylsilyl)ethynyl-1,10-phenanthroline (phenC≡$CSiMe_3$) or 3,8-di[(tri-

(11) (a) Sullivan, B. P.; Salmon, D. J.; Meyer, T. J. *Inorg. Chem.* **1978**, *17*, 3334. (b) Hadda, T. B.; Bozec, H. L. *Inorg. Chim. Acta* **1993**, *204*, 103. (c) Lai, S.-W.; Chan, M. C. W.; Cheung, K.-K.; Che, C.-M. *Inorg. Chem.* **1999**, *38*, 4262. (d) Connors, P. J., Jr.; Tzalis, D.; Dunnick, A. L.; Tor, Y. *Inorg. Chem.* **1998**, *37*, 1121. (e) Tzalis, D.; Tor, Y. *J. Am. Chem. Soc.* **1997**, *119*, 852.
(12) Crosby, G. A.; Demas, J. N. *J. Phys. Chem.* **1971**, *75*, 991.
(13) Sheldrich, G. M. *SHELXL-97, Program for the Refinement of Crystal Structures*; University of Göttingen: Göttingen, Germany, 1997.

Scheme 1

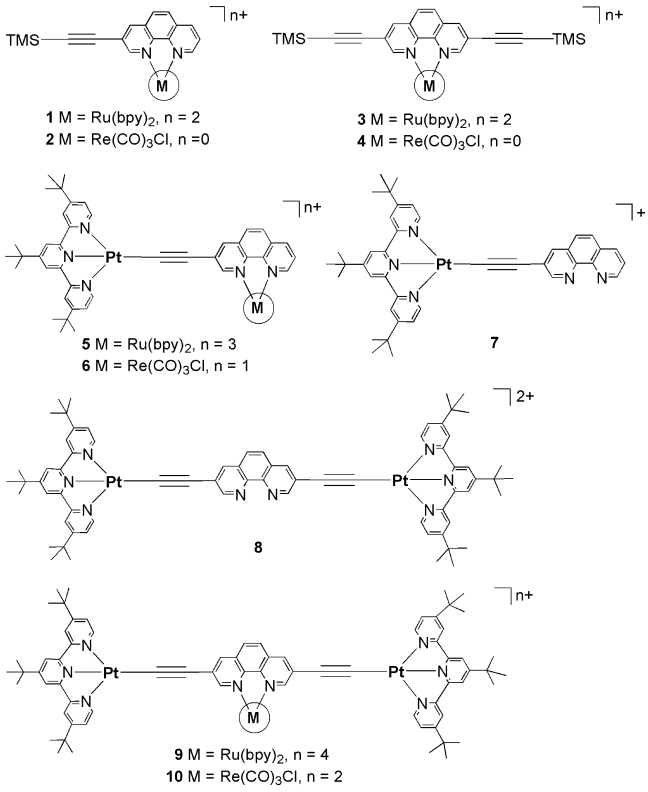

methylsilyl)ethynyl]-1,10-phenanthroline($Me_3SiC{\equiv}CphenC{\equiv}CSiMe_3$) was prepared by the reaction of 3-bromo-1,10-phenanthroline or 3,8-dibromo-1,10-phenanthroline with (trimethylsilyl)acetylene though the Sonogashira coupling reaction using $Pd(PPh_3)_2Cl_2$ and CuI as catalysts.[14] The reaction of *cis*-$Ru(bpy)_2Cl_2{\cdot}2H_2O$ or $Re(CO)_5Cl$ with $phenC{\equiv}CSiMe_3$ or $Me_3SiC{\equiv}CphenC{\equiv}CSiMe_3$ under refluxing ethanol or toluene solutions gave the corresponding mononuclear Ru^{II} or Re^{I} compounds **1**−**4** in 70–75% yield through ruthenium or rhenium phenanthroline chelation. The analogous of the mononuclear Ru^{II} and Re^{I} complexes **1**−**4** containing −C≡CH instead of $-C{\equiv}CSiMe_3$ groups have already been described in the literature.[3h,11d,e] The platinum(II) terpyridyl alkynyl species **7** or **8** was synthesized by the coupling reaction of $[Pt(^tBu_3tpy)Cl](PF_6)$ with $phenC{\equiv}CSiMe_3$ or $Me_3SiC{\equiv}CphenC{\equiv}CSiMe_3$ catalyzed by CuI via fluoride-promoted desilylation in the presence of KF in a refluxing dichloromethane−methanol solution [2:1 (v/v)].[6d] Utilizing the mononuclear Ru^{II} or Re^{I} compounds **1**−**4** as precursors, the reactions with $[Pt(^tBu_3tpy)Cl](PF_6)$ induced successful isolation of the Pt−Ru and Pt−Re heteronuclear complexes **5**, **6**, **9** and **10** (Scheme 1) through platinum acetylide σ coordination catalyzed by CuI.

These complexes (Scheme 1) were characterized by ESI-MS spectrometry, ^1H NMR and IR spectroscopy, and elemental analyses and by X-ray crystallography for **9**. The microanalytical data of C, H, and N contents coincided well with the calculated ones. The positive-ion ESI-MS spectra revealed that the molecular ion fragments $[M]^+$ for **2** and **4**, $[M - PF_6]^+$ for **6** and **7**, $[M - 2PF_6]^{2+}$ for **1**, **3**, **8**, and **10**, $[M - 3PF_6]^{3+}$ for **5**, and $[M - 4PF_6]^{4+}$ for **9** occur as base peaks or principal peaks with high abundances. Typical $\nu(C{\equiv}C)$ vibrational bands occur at ca. 2160 cm^{-1} in the IR spectra of Ru^{II} or Re^{I} mononuclear precursors **1**−**4**. These $\nu(C{\equiv}C)$ frequencies are obviously shifted to 2110–2120 cm^{-1} upon formation of platinum acetylide σ bonding in **5**−**10**. Moreover, the Re^{I} compounds **2**, **4**, **6**, and **10** show three strong $\nu(CO)$ bands at 1880–2030 cm^{-1}, agreeing well with the facial arrangement of the three CO around the Re^{I} center.[3e,h]

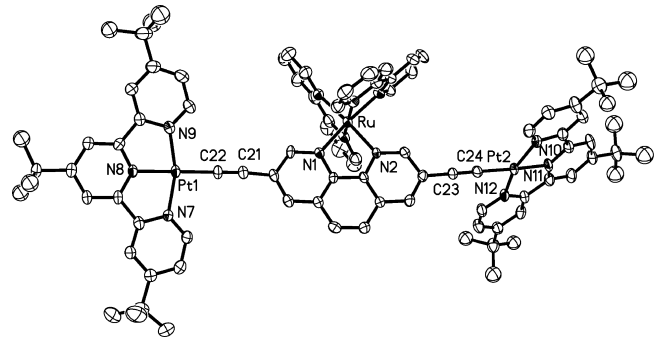

Figure 1. ORTEP drawing of the complex cation of **9** with an atom-labeling scheme showing 30% thermal ellipsoids.

Table 2. Selected Bond Lengths (Å) and Angles (deg) for **9**

Pt1−N7	2.008(7)	Pt2−N10	2.016(7)
Pt1−N8	1.961(6)	Pt2−N11	1.957(7)
Pt1−N9	2.005(7)	Pt2−N12	2.016(7)
Pt1−C22	1.977(8)	Pt2−C24	1.965(8)
C21−C22	1.196(11)	C23−C24	1.198(11)
Ru−N1	2.080(6)	Ru−N2	2.060(6)
Ru−N3	2.061(7)	Ru−N4	2.057(7)
Ru−N5	2.057(7)	Ru−N6	2.060(8)
N8−Pt1−N9	80.6(3)	N9−Pt1−N7	160.8(3)
C21−C22−Pt1	178.6(8)	N11−Pt2−N10	80.2(3)
N10−Pt2−N12	161.1(3)	C23−C24−Pt2	170.4(8)
N5−Ru−N4	94.0(3)	N5−Ru−N6	79.5(3)
N4−Ru−N6	172.6(3)	N5−Ru−N2	93.2(2)
N4−Ru−N2	95.1(3)	N6−Ru−N2	88.7(3)
N5−Ru−N3	89.3(3)	N4−Ru−N3	78.5(3)
N6−Ru−N3	97.9(3)	N2−Ru−N3	173.3(3)
N5−Ru−N1	171.3(3)	N4−Ru−N1	91.8(3)
N6−Ru−N1	95.0(3)	N2−Ru−N1	79.8(2)
N3−Ru−N1	98.3(3)		

Crystal Structure. An ORTEP drawing of the complex cation of **9** is depicted in Figure 1. Selected bond distances and angles are listed in Table 2. The complex cation exhibits a PtRuPt heterotrinuclear array composed of two $Pt(^tBu_3tpy)$(acetylide) subunits and one $Ru(bpy)_2(phen)$ chromophore, in which 3,8-diethynyl-1,10-phenanthroline serves as a bifunctional bridging ligand associated with both $Pt(^tBu_3tpy)$ subunits through platinum acetylide σ bonding and the $Ru(bpy)_2$ component through ruthnium phenanthroline chelation. The Pt^{II} centers exhibit a distorted square-planar environment built by a σ-coordinated C donor from the acetylide and terdentate N_3 donors from the chelated terpyridyl. The N−Pt−N angles deviate from the ideal values of 90° and 180° due to the steric requirement of the terpyridine ligand, which is consistent with that found in other platinum(II) terpyridyl alkynyl complexes.[4a,5b,c,9a] The Pt−C≡C angles are close to 180° with C21−C22−Pt1 = 178.61° and

(14) (a) Schmittel, M.; Michel, C.; Wiegrefe, A.; Kalsani, V. *Synthesis* **2001**, 1561. (b) Ziessel, R.; Stroh, C. *Tetrahedron Lett.* **2004**, *45*, 4051.

Table 3. Absorption and Electrochemical Data in Acetonitrile for **1**–**10**

complex	λ_{abs}/nm (ϵ/M^{-1} cm^{-1})[a]	E_{ox}[b] (V)	E_{red}[b] (V)	ΔE[c] (V)
1	281 (85 230), 328 (20 490), 430 (13 590), 450 (14 320)	+0.95	−1.58	2.53
2	281 (48 960), 316 (27 980), 390 (4580)	+0.98	−1.59	2.57
3	285 (95 450), 341 (36 890), 436 (13 080), 480 (9550)	+1.01	−1.47	2.48
4	274 (45 930), 350 (32 620), 400 (3340)	+1.00	−1.43	2.43
5	286 (89 050), 352 (29 530), 426 (13 810), 448 (14 950)	+0.96	−1.34	2.30
6	284 (48 960), 336 (32 570), 400 (13 700)	+1.01	−1.37	2.38
7	283 (54 670), 322 (36 380), 405 (15 450)	+1.06	−1.33	2.39
8	284 (92 870), 337 (68 560), 432 (21 220)	+1.00	−1.34	2.34
9	285 (82 370), 338 (34 980), 410 (42 890), 451 (21 950)	+1.02	−1.33	2.35
10	284 (44 490), 335 (28 850), 407 (24 990)	+1.02	−1.35	2.37

[a] Measured in acetonitrile at room temperature. [b] Potential data in volts versus Fc^+/Fc are from a single scan cyclic voltammogram recorded at 25 °C in a 0.1 M acetonitrile solution of Bu_4NPF_6. [c] $\Delta E = E_{ox} - E_{red}$.

C23−C24−Pt2 = 170.46°, showing the quasi-linear connection between the platinum(II) terpyridyl moieties and the alkynyl through σ-acetylide coordination. The Pt−C (1.965 and 1.977 Å) and C≡C (1.196 and 1.198 Å) bond distances are in the normal range for platinum(II) alkynyl complexes.[4a,5b,c,9a] The Ru^{II} center exhibits a typically pseudooctahedral geometry composed of N_6 donors with the Ru−N (2.057–2.080 Å) bonds distances comparable to those in the $[Ru(diimine)_3]^{2+}$ complexes.[15] The Pt−Ru distances are 8.18 and 8.55 Å, whereas the Pt−Pt separation across the bridging 3,8-diethynyl-1,10-phenanthroline is ca. 15.94 Å. The shortest intermolecular Pt−Pt distance is longer than 4.2 Å, excluding the possibility to form Pt−Pt contacts. The square-planar coordination planes of Pt1 and Pt2 centers are nonplanar so as to form a dihedral angle of 50.1°.

Electrochemical Properties. The electrochemical data of **1**–**10** are summarized in Table 3. The mononuclear Ru^{II} complexes exhibit a quasi-reversible Ru-based oxidation wave at ca. +0.95 V for **1** and +1.01 V for **3**. Compared with the Ru-centered oxidation potential (+0.89 V vs Fc/Fc^+) for $[Ru(bpy)_3]^{2+}$,[16] the corresponding oxidation potentials for **1** (0.95 V) and **3** (1.01 V) are slightly anodic-shifted because of the better π-accepting capability of 1,10-phenanthrolinealkynyl ligands relative to that of bpy.[17] The first ligand-centered reduction potential is ca. −1.58 V for **1** and −1.47 V for **3**, which is much less negative than the first bpy-based reduction for $[Ru(bpy)_3]^{2+}$ (−1.72 V).[16] This suggests that the first reduction for **1** and **3** is probably caused by the 1,10-phenanthrolinealkynyl ligand because of the better π-accepting capability in comparison with that of the bpy ligand. The less negative 1,10-phenanthrolinealkynyl-centered reduction potential for **3** (−1.47 V) than that for **1** (−1.58 V) can be assigned to the more extended π conjugation in 3,8-diethynyl-1,10-phenanthroline than that in 3-ethynyl-1,10-phenanthroline. The mononuclear Re^I complexes show an irreversible Re-centered oxidation at ca. 0.98 V for **2** and 1.00 V for **4**.[3e] The first 1,10-phenanthrolinealkynyl-based reduction occurs at ca. –1.59 V for **2** and −1.43 V for **4**, which are comparable to those for **1** and **3**. This further confirms that the first reduction process is resident on the 1,10-phenanthrolinealkynyl ligands in both mononuclear Ru^{II} (**1** and **3**) and Re^I (**2** and **4**) complexes.

The mononuclear Pt^{II} complexes **7** and **8** exhibit an irreversible Pt-based oxidation wave at ca. +1.0 V. The first reduction potential at ca. −1.30 V is ascribable to the terpyridyl-based reduction as found in related platinum(Π) terpyridyl alkynyl complexes.[4a,9a,b] For the PtM [M = Ru (**5**), Re (**6**)] and Pt_2M [M = Ru (**9**), Re (**10**)] heteronuclear complexes, only one quasi-reversible (for M = Ru) or irreversible (for M = Re) oxidation wave occurs at 0.96–1.02 V because of probably the severe overlapping of both Pt- and Ru/Re-centered redox waves. The first reduction potentials of these heteronuclear species are also comparable to those in the Pt- and Ru/Re-based precursors (Table 3).

UV–Vis Absorption Spectra. The UV–vis absorption spectral data of **1**–**10** are presented in Table 3. The intense high-energy bands below 300 nm are ascribable to ligand-centered transitions,[3,4,17] whereas the medium-energy absorption at 310–350 nm is likely due to the acetylide $\pi \rightarrow \pi^*$(C≡C) transition.[3f,h,4,17] The low-energy absorption at 390–480 nm arises most likely from Ru-, Re-, and/or Pt-based MLCT transitions, mixed probably with some π(C≡Cphen) → $\pi^*(^tBu_3tpy)$ ligand-to-ligand charge-transfer (LLCT) character for Pt^{II} complexes.[3e,f,h,4,8,16,17]

As indicated in Table 3, both the medium-energy bands due to $\pi \rightarrow \pi^*$(C≡C) transitions and the low-energy absorptions due to MLCT/LLCT states are much stronger and obviously red-shifted in the diethynyl complex **3** or **4** than those in the corresponding monoethynyl counterpart **1** or **2**, ascribable to the more extended π system in the former compared with that in the latter.[4a,17c] In contrast to the weaker low-energy absorption from dπ(Re) → π^*(phen) transition in mononuclear Re^I complex **2** or **4**, the broad and low-energy absorption due to dπ(Ru) → π^*(phen/bpy) MLCT states is significantly stronger in mononuclear Ru^{II} species **1** or **3**.[16]

Compared with that in the mononuclear Pt^{II} species **7** (322 nm), the absorption from intraligand $\pi \rightarrow \pi^*$(C≡C) transitions is significantly stronger and obviously red-shifted in the diplatinum complex **8** (337 nm), where the molar extinction coefficient in **8** (ϵ = 68 560 M^{-1} cm^{-1}) is almost twice that in **7** (ϵ = 36 380 M^{-1} cm^{-1}) because of the double number of platinum ethynyl units in **8**. Furthermore, the low-energy absorption due to the dπ(Pt) → $\pi^*(^tBu_3tpy)$ MLCT state mixed probably with some π(C≡Cphen) → $\pi^*(^tBu_3tpy)$

(15) Rillema, D. P.; Jones, D. S.; Levy, H. A. *J. Chem. Soc., Chem. Commun.* **1979**, 849.
(16) Shavaleev, N. M.; Bell, Z. R.; Easun, T. L.; Rutkaite, R.; Swanson, L.; Ward, M. D. *Dalton Trans.* **2004**, 3678.
(17) (a) Glazer, E. C.; Magde, D.; Tor, Y. *J. Am. Chem. Soc.* **2005**, *127*, 4190. (b) Glazer, E. C.; Magde, D.; Tor, Y. *J. Am. Chem. Soc.* **2007**, *129*, 8544. (c) Tzalis, D.; Tor, Y. *Chem. Commun.* **1996**, 1043.

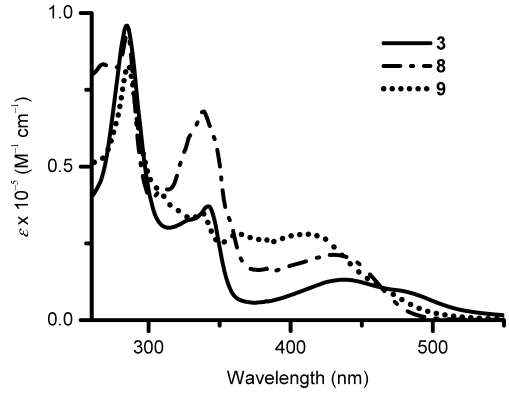

Figure 2. UV–vis absorption spectra of **3** (Ru), **8** (Pt_2), and **9** (Pt_2Ru) in acetonitrile solutions at room temperature.

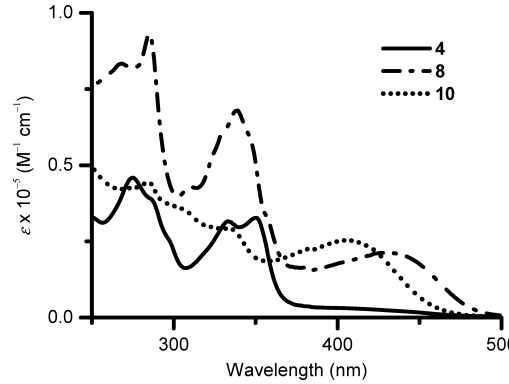

Figure 3. UV–vis absorption spectra of **4** (Re), **8** (Pt_2), and **10** (Pt_2Re) in acetonitrile solutions at room temperature.

LLCT character is also distinctly red-shifted from **7**(405 nm) to **8** (432 nm). Relative to that of the bridging ligand 3-ethynyl-1,10-phenanthroline in **7**, the π-donor orbital energy of the bridging ligand 3,8-diethynyl-1,10-phenanthroline in **8** is raised as predicted from the Hückel molecular orbital theory.[19] Because the increased π-donor orbital energy of the bridging ligand 3,8-diethynyl-1,10-phenanthroline in **8** would raise the energy level of the dπ(Pt) orbital through pπ−dπ overlap, the energy gap between the highest occupied molecular orbital (HOMO) [dπ(Pt)] and lowest unoccupied molecular orbital (LUMO) [π^*(^{t}Bu$_3$tpy)] would be reduced, thus inducing a red shift of the MLCT absorption in diplatinum(II) complex **8** compared with that in Pt^{II} mononuclear species **7**.[4a,18d] The same phenomenon is also observed by comparison of the absorption features in the PtM (M = Ru or Re) heterobinuclear monoethynyl species (**5** or **6**) with those in the corresponding Pt_2M heterotrinuclear diethynyl complexes (**9** or **10**), in which the absorptions due to dπ(Pt) → π^*(^{t}Bu$_3$tpy) MLCT states in the heterotrinuclear species **9** or **10** are significantly stronger and red-shifted than those in the heterobinuclear complex **5** or **6**.

Because of the presence of both Pt(^{t}Bu$_3$tpy)(acetylide) and Ru(bpy)$_2$(phen)/Re(phen)(CO)$_3$Cl chromophores in PtRu (**5**) or PtRe (**6**) diads and Pt_2Ru (**9**) or Pt_2Re (**10**) triads, the broad and low-energy absorptions in the near-visible region originate probably from an admixture of both dπ(Pt) → π^*(^{t}Bu$_3$tpy) and dπ(Ru/Re) → π^*(bpy/phen) MLCT states, in which the Pt-based MLCT absorption is localized at a higher energy than that from the Ru/Re-based MLCT state, as indicated in Figures 2 and 3. In comparison with those of the corresponding Pt^{II}-only (**7** and **8**) and Ru^{II}-only (**1** and **3**) precursors, both Pt- and Ru-based MLCT absorptions are obviously blue-shifted to a higher energy in the PtRu (**5**) or Pt_2Ru (**9**) heteronuclear species, as depicted in Figure 2. On the one hand, the blue shift of Pt-based MLCT absorption is readily understandable because the formation of the PtRu (**5**) or Pt_2Ru (**9**) array from the mono- (**7**) or dinuclear (**8**) Pt^{II} species by complexation of one Ru(bpy)$_2$ subunit through 1,10-phenanthroline chelation would lower the energy level of the bridging C≡Cphen or C≡CphenC≡C, thus reducing the energy level of the dπ(Pt) orbital and consequently increasing the energy gap between dπ(Pt) and π^*(^{t}Bu$_3$tpy) orbitals in the dπ(Pt) → π^*(^{t}Bu$_3$tpy) MLCT transition. On the other hand, the formation of the PtRu diad **5** or Pt_2Ru triad **9** by introducing one or two π-electron-accepting [Pt(^{t}Bu$_3$tpy)]$^{2+}$ subunits to the mononuclear Ru^{II} precursor **1** or **3** through platinum acetylide σ coordination would reduce the electron density in the phenC≡C or C≡CphenC≡C ligand and subsequently that in the Ru^{II} center, thus lowering the energy level of the dπ(Ru) orbital (HOMO) and increasing the HOMO–LUMO energy gap in the dπ(Ru) → π^*(bpy/phen) MLCT transition. For the PtRe (**6**) or Pt_2Re (**10**) species (Figure 3), the weaker Re-based MLCT absorption is severely covered by the intense Pt-based MLCT absorption, which is obviously blue-shifted compared with that in the Pt^{II} precursor **7** or **8** for the same reason as mentioned above.

Table 4. Luminescence Data of **1**–**10**

	acetonitrile		solid
complex	λ_{em}/nm (τ_{em}/μs)[a]	φ_{em} (%)[b]	λ_{em}/nm (τ_{em}/μs)
1	625 (0.86)	5.97	633 (0.43)
2	625 (0.03)	0.73	593 (0.48)
3	655 (0.80)	5.86	657 (1.17)
4	660 (0.008)	0.27	612 (0.13)
5	607 (0.38)	6.32	614 (0.12)
6	600 (0.12, 0.60)	0.93	548 (1.32), 589 (0.34)
7	531 (0.57)	2.55	576 (0.58)
8	560 (0.51)	5.03	597 (0.29)
9	610 (0.86)	6.58	624 (1.53)
10	570 (0.36), 610sh (1.80)	0.72	567 (1.11), 608sh (0.26)

[a] In degassed acetonitrile at 298 K. [b] The quantum yields in degassed MeCN were determined relative to that of [Ru(bpy)$_3$](PF$_6$)$_2$ (bpy = 2,2′-bipyridine) in degassed CH_3CN as the standard (φ_{em} = 0.062).

Luminescence Properties. The luminescence data of **1**−**10** are summarized in Table 4. These complexes show intense room-temperature luminescence in both solid states and degassed acetonitrile solutions with a submicrosecond range of lifetimes, revealing that they are characteristic of triplet excited states. The emission quantum yields in degassed acetonitrile solutions are in the range 0.27–6.58% at ambient temperature.

Upon excitation at λ_{ex} > 350 nm, the mononuclear Ru^{II} complexes **1** and **3** luminesce strongly at 625–660 nm,

(18) (a) Striplin, D. R.; Crosby, G. A. *Coord. Chem. Rev.* **2001**, *211*, 163. (b) Schanze, K. S.; MacQueen, D. B.; Perkins, T. A.; Cabana, L. A. *Coord. Chem. Rev.* **1993**, *122*, 63. (c) Juris, A.; Balzani, V.; Barigelletti, F.; Campagna, S.; Belser, P.; von Zelewsky, A. *Coord. Chem. Rev.* **1988**, *84*, 85. (d) Yam, V. W.-W.; Lau, V. C.-Y.; Cheung, K.-K. *Organometallics* **1996**, *15*, 1740.
(19) Hoffmann, R. *Tetrahedron* **1966**, *22*, 521.

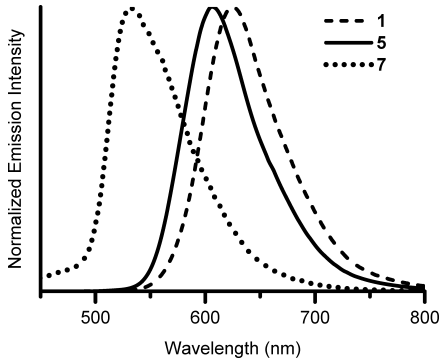

Figure 4. Emission spectra of **1** (Ru), **5** (PtRu), and **7** (Pt) in degassed acetonitrile solutions at room temperature (λ_{ex} = 400 nm).

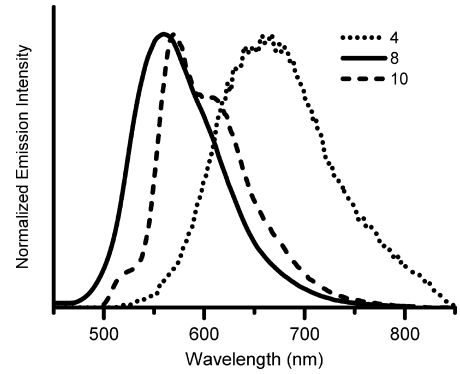

Figure 5. Emission spectra of **4** (Re), **8** (Pt_2), and **10** (Pt_2Re) in degassed acetonitrile solutions at room temperature (λ_{ex} = 400 nm).

induced by the dπ(Ru) → π*(bpy/phen) ^{3}MLCT state. Irradiation of the mononuclear Re^I complexes **2** and **4**, however, results in much weaker luminescence ascribed to the dπ(Re) → π*(phen) ^{3}MLCT state, although the emission energy is comparable to that in the corresponding Ru^{II} counterparts.[3j,l,16–18] The much higher quantum yields for the Ru^{II} complexes in comparison with those for the corresponding Re^I species are probably attributed to the more effective intersystem crossing between the singlet and triplet states to populate the ^{3}MLCT state for the Ru^{II} complexes.[3j,16,18] The emission of diethynyl complexes **3** (655 nm) and **4** (660 nm) occurs at lower energy compared with that of monoethynyl species **1** (625 nm) and **2** (625 nm) because the more extended π conjugation in $Me_3SiC{\equiv}CphenC{\equiv}CSiMe_3$ species would lower the energy level of the π*(phen) orbital (LUMO), thus inducing a smaller energy gap between the HOMO and LUMO in the corresponding ^{3}MLCT transition.[17,19] Noticeably, the luminescence of Pt^{II}-only complexes **7** and **8** (530–560 nm) likely due to the dπ(Pt) → π*(^{t}Bu$_3$tpy) ^{3}MLCT state[4,6] occurs at much higher energy than that in Ru^{II}/Re^I-only species **1**−**4**. Likewise, because of the more extended π system in the diplatinum species **8**, it exhibits a lower energy emission compared with that in the mononuclear Pt^{II} complex **7**.

As indicated in Table 4, the luminescence of Pt_2Ru heterotrinuclear complex **9** occurs at a slightly lower energy than that of PtRu heterobinuclear complex **5** in both solid states and fluid acetonitrile solutions because of the more extended π conjugation in the former. Noticeably, their luminescence parameters (Table 4) including emissive energy, lifetime, and quantum efficiency are comparable to those of the mononuclear Ru^{II} precursors **1** and **3** but far from those of the mono- and dinuclear Pt^{II} precursors **7** and **8**. Consequently, the luminescence of **5** and **9** arises most likely from the Ru-based ^{3}MLCT excited states, whereas the Pt-based emission is mostly quenched owing to quite efficient energy transfer from the Pt-based ^{3}MLCT excited states to the Ru-based ^{3}MLCT states in the Pt−Ru heterometallic arrays. As indicated in Figure 4, the emission of **5** (PtRu) or **9** (Pt_2Ru) from the Ru-based ^{3}MLCT state is obviously blue-shifted compared with that of the Ru^{II}-only mononuclear precursor **1** or **3**. The blue shift of the Ru-based ^{3}MLCT emission energy is consistent with that observed in the absorption spectra. Formation of the PtRu diad **5** or the Pt_2Ru triad **9** by complexation of one or two π-electron-accepting $[Pt(^tBu_3tpy)]^{2+}$ subunits to the mononuclear Ru^{II} precursor **1** or **3** through platinum acetylide σ coordination would reduce the π-donating ability in the phenC≡C or C≡CphenC≡C ligand and subsequently the electron density in the Ru^{II} center, thus lowering the energy level of the dπ(Ru) orbital (HOMO) and increasing the HOMO–LUMO energy gap in the Ru-based ^{3}MLCT excited state.

For the Pt−Re heteronuclear arrays, although the emission profile of **6** (PtRe) is broad with a maximum at 600 nm, the emission spectrum of the Pt_2Re complex **10** (Figure 5) shows distinctly a dual emission at 570 and 610 nm owing probably to the Pt- and Re-based MLCT states, respectively. The lifetimes of both **6** and **10** are best described by a biexponential fitting, suggesting further that two possible emissive states are operating in the Pt−Re species. The room-temperature quantum yields of **6** (0.93%) and **10** (0.72%) in degassed acetonitrile are much lower than those of the Pt^{II} precursors **7** (2.55%) and **8** (5.03%) but close to those of the Re^I precursors **2** (0.73%) and **4** (0.27%). This together with the much higher emissive energy for the Pt-based ^{3}MLCT state than that for the Re-based state suggests that energy transfer is most likely operating from the Pt-based MLCT chromophores to the Re-based ^{3}MLCT emitter, which induces a significant emission quenching for the Pt-based ^{3}MLCT state in the Pt−Re heteronuclear species. Therefore, although Pt → Re energy transfer in the Pt−Re heteronuclear species is not as efficient as that of Pt → Ru energy transfer in the PtRu or Pt_2Ru heteronuclear complexes, the emission in **6** (PtRe) and **10** (Pt_2Re) is primarily from the Re-based dπ(Re) → π*(phen) ^{3}MLCT state, mixed with some character from the Pt-based dπ(Pt) → π*(^{t}Bu$_3$tpy) ^{3}MLCT transition.

Conclusions

A series of PtM and Pt_2M (M = Ru^{II}, Re^I) heteronuclear complexes with 3-ethynyl-1,10-phenanthroline (HC≡Cphen) or 3,8-diethynyl-1,10-phenanthroline (HC≡CphenC≡CH) were prepared by introducing both $Ru(bpy)_2$/$Re(CO)_3Cl$ (bpy = 2,2′-bipyridyl) and Pt(^{t}Bu$_3$tpy) (4,4′,4″-tri-*tert*-butyl-2,2′:6′,2″-terpyridine) subunits through ruthenium (rhenium) phenanthroline chelation and platinum acetylide σ coordination, respectively. The stepwise complexation of different types of metal components to 1,10-phenanthroline-functionalized ethynyl ligands affords a feasible approach for

construction of the desired multicomponent species through elaborately organized photoactive and/or electroactive transition-metal subunits.

These Pt−Ru and Pt−Re complexes exhibit intense room-temperature luminescence in both solid states and fluid solutions with lifetimes in the submicrosecond scale and quantum yields (φ_{em}) in the range 0.27–6.58%. For the Pt−Ru complexes, the luminescence is characteristic of a Ru^{II}-based ^{3}MLCT state, whereas the emission from a Pt^{II}-based triplet excited state is mostly quenched because of quite effective intramolecular Pt → Ru triplet energy transfer from the platinum(II) terpyridyl acetylide chromophores to the Ru^{II}-based acceptor. The Pt−Re species, however, display a dual-luminescence feature dominated by a $d\pi$(Re) → π^*(phen) triplet excited state mixed with some $d\pi$(Pt) → π^*(^{t}Bu$_3$tpy) character, in which the Pt-based emission is partially quenched because of intercomponent Pt → Re energy transfer from the Pt^{II}-based chromophores to the Re^{I}-based emitters. Compared with those in the PtRu or PtRe heterodinuclear complexes, both absorption and emission are red-shifted in the corresponding Pt_2Ru or Pt_2Re heterotrinuclear species because of the more extended π conjugation in the heterotrinuclear systems.

Acknowledgment. This work was supported financially by the NSFC (Grants 20490210, 20521101, 20625101, and 20773128), the 973 project (Grant 2007CB815304) from MSTC, the NSF of Fujian Province (Grant E0420002), and the Key Project from CAS (Grant KJCX2-YW-H01).

Supporting Information Available: Additional absorption (Figures S1−S4) and emission spectra (Figures S5 and S6) and an X-ray crystallographic file in CIF format for the structure determination of **9**. This material is available free of charge via the Internet at http://pubs.acs.org.

IC702055N